Impact Assessment of Land Use and Land Cover Change on the Runoff Changes on the Historical Flood Events in the Laigiang River Basin of the South Central Coast Vietnam

Ngo, A.T.,[1*] Grivel S.,[2] Nguyen, T.D.[1] and Nguyen, T.T.V.[1].
[1]Faculty of Natural Sciences, Quynhon University, 170 An Duong Vuong Street, Quynhon City, 55000 Binhdinh, Vietnam
E-mail: ngoanhtu@qnu.edu.vn,* nguyentrongdoi@qnu.edu.vn, nguyenthituongvi@qnu.edu.vn
[2]AgroParisTech, Paris-Saclay University, 16 Rue Claude Bernard, 75005 Paris, France
E-mail: stephane.grivel@agroparistech.fr
Corresponding Author

DOI: https://doi.org/10.52939/ijg.v19i9.2881

Abstract
It is crucial for effective flood events management in a river basin that the relationship between land use, land cover (LULC) changes and peak flow. The flood in Central Vietnam got highly affected in recent decades due to several factors like deforestation, urbanization, lack of hydrometeorological stations, developmental monitoring and planning. This study quantifies the influence of LULC on the peak flow dynamics using a hydrological model, remote sensing technology in the Laigiang river basin. The responses of LULC changes on the peak flow and runoff volume were investigated using daily rainfall in December 2016 at the study area. The usage of the hydrological model defined that the changes in LULCs 2010-2020 caused momentous changes in hydrological response towards water flow. The rainy season floods in the bare land, low-density vegetation area, urban/built-up, and bare land while the normal flow gets the contribution from interflow generated from the dense forest.

Keywords: Flood Events, Hydrological Modeling, Land Cover Changes, Lai Giang River, Vietnam

1. Introduction

In the past recent years, the weather has changed very complicatedly, causing floods and droughts which happened with increasing frequency and intensity, all linked to Global climate change [1]. This has threatened the process of stable and sustainable development for the world, especially in tropical countries. A flood can be confirmed in each river basin where is affected by the combined effects of factors such as rainfall, area of the basin, slope, elevation, land cover, and land use [2] [3] [4] and [5]. However, the influence of these factors on flooding in the river basin is not the same [6] and [7]. In particular, forests play a very important role in regulating water sources, reducing surface runoff and transferring rainwater infiltration into the ground. It is increasingly acknowledged that the impact of the change of land cover/land use (LULC) on the hydrological cycle of the basin has become a topic of great interest in the study of global environmental change [8] [9] and [10].

Many researches in other parts of the world studied to quantify the impact of deforestation [3] [11] and [12], natural forest conversion and degradation [13], Dams [4], forest road network construction status [14], urbanized river basins [15] which have affected the flow during the wet and dry seasons of the river basins.

Vietnam is located in southeastern Asia, due to differences in latitude and in topographical relief, unfavourable local meteorological conditions coupled with global climate change have increased annual rainfall, mainly during a short period in the rainy season [16]. From 1999 to now, there was 10 worst flood events have occurred in Vietnam, of which the Central region accounts for 70%. There are many causes of floods, in which the change in LULC (the forest is rapidly decreasing in area and quality of forest), effects of urban development, extreme climate events and climate change which has caused floods to appear more and more [17].

ISSN: 1686-6576 (Printed) | ISSN 2673-0014 (Online) |

LULC volatility detection is the process of identifying a change in the state of an object or a phenomenon by observing it at various times [18]. This is considered an important process in natural resource monitoring and management because it provides quantitative analysis results of the spatial distribution of the object of interest. Over the years, Remote Sensing technology (RS), Geographic Information System (GIS), and hydrological modeling which has become popular and widely applied in LULC research and determining the changing effects of LULC on river basin discharge [19] [20] [21] and [22]. Especially, the combination of RS and GIS can be improved on LULC determination (past and present). Furthermore, GIS intelligence helps to improve the ability to identify river basin morphology as well as determine the average rainfall of the river basin accurately.

Research on how LULC affects flood peak discharges and runoff volumes in river basins needs to be multidisciplinary and interdisciplinary. Therefore, the aim of the paper is to use satellite images of Landsat from of the period 2010-2020, and integrating GIS with hydrological modeling (HEC-HMS) to assess the effects of urbanization, deforestation, degraded forest quality as well as changing crop structure that has affected increases in the flood volume and peak of discharge in the Laigiang river basin of the South Central Coast Vietnam. To achieve this, historical of the period 2010-2020 LULC trends were analysed; LULC scenarios of flood event in December 2016 were simulated using the HEC-HMS model.

2. Materials and Methods

2.1 Study Area

The study area (Figure 1) is the Lai Giang River basin located in the South Central Coast of Vietnam, which has a catchment area of about 1,466 km^2 that lies between 14° 25′ 46″ N latitude and 108° 57′ 15″E longitude.

Figure 1: Location of the study area

ISSN: 1686-6576 (Printed) | ISSN 2673-0014 (Online) | © Geoinformatics International

The study area falls under the tropical monsoon climate type, the mean annual rainfall is 2,500.0 mm. This river basin is exposed to experiencing characteristically regular flooding due to the prolonged rainfall events, usually associated with typhoons, and combine short and steep terrain. Furthermore, the hydrological functioning of the Lai Giang basin is poorly known because there are no hydrological models and not enough flow measurements. For the period 1980 to 2019, the Laigiang river basin has recorded a number of major floods such as 11/1980, 10/1990, 9/2009, 12/2016, and 12/2019s. In which, the flood from 15th to 16th December 2016 is an assessed historical flood event with 44 of lives lost. The property was also severely impacted, with 908 houses destroyed and 409 submerged in flood. According to Binh Dinh disaster management authority, economic losses from the flood-related in the river basin reached around an 85 million euros over the past 50 years.

2.2 Data Collection

The main data used in the study is Landsat 5 Thematic Mapper (TM) and Landsat 8 Operational Land Imager (OLI) with 8 spectral bands (band 1-7 and 9) with a spatial resolution of 30 m acquired on 30/07/2010, 30/06/ 2015, and 09/07/2020 from the https://earthexplorer.usgs.gov/. Besides, Digital Elevation Model (DEM) is useful in this study, such as delineate hydrological networks, delineating watersheds and defining a catchment area. This DEM currently contains of the Alaska Satellite Facility (ASF) data in spatial resolution 12.5m from the https://search.asf.alaska.edu/#/. Hydrological data: data such as daily rainfall data, water level, and runoff are collected from the Binh Dinh Meteorological Department of Vietnam in 2016. In which, in the Laigiang river basin, there is only 01 flow measuring station, namely Anhoa, two water level monitoring stations, and three rainfall stations and namely: Anhoa, Hoaian, and Bongson wich are also collected in 2016. In addition, the study has consulted data about Laigiang river's constant monthly baseflow offered by [23]. The baseflow is 28.6 m3/s of December 2016 at the study area. Cross-sectional data of main channel: there were 19 created river cross-sections from upstream to downstream of Laigiang river in 2016 with a direct measurement method by using the RTK GPS Trimble R4. Soil data: this data, also collected by us from the Vietnam Soil and Terrain at a scale ratio 1: 200,000 in 2010. This soil data ware used to define infiltration parameters for rainfall runoff modeling within HEC-HMS.

2.3 Methodology

In this study, the Hydrological Engineering Center - Hydrological Modelling System (HEC-HMS) model using Soil Conservation Service (SCS) curve number (CN) [24] model is used to study the significant impact of land use/land cover (LULC) changes (2010-2020) on severe water flow events in the Laigiang River basin during December 2016 [25]. Flood estimation was executed in view of the daily rainfall scale.

2.3.1 Satellite images were classified to produce LULC assessment

The study had done using Landsat imageries to identify changes in LULC distribution in the Laigiang river basin in the period of 2010 - 2020. These Landsat imageries are corrected for coordinates, topographic correction, image enhancement, and cloud filtering [26]. Then, the LULC features are extracted using Landsat acquired in 2010, 2016, and 2020 with the maximum likelihood for supervised image classification [27]. In addition, the images provided complete coverage of the study area and stacking of bands, sub-setting of the images had done using the QGIS 3.18 software. The Kappa coefficient proposed by [28] is to be used to determine accuracy [29].

Mean area precipitation: Rainfall data of measuring observations in or contiguous to the catchment has been used to calculate the average rainfall in the basin. The Thiessen polygon was used to obtain the areal average precipitation [30]. The mean area precipitation has been calculated by the following Equation 1.

$$X_m = \frac{\sum_i \left(w_i \sum_i x_i(t) \right)}{\sum_i x_i}$$

Equation 1

where: X_m is mean area precipitation; $x_i(t)$ is precipitation measured at time t at station i; and w_i is weighting factor assigned to station i.

2.3.2 HEC-HMS program

HEC-HMS uses a separate model to represent each part of the runoff process, including: Runoff-volume model, direct-runoff model, baseflow model, and routing model.

Runoff-volume model: The SCS curve number (CN) model is selected to be used to estimate precipitation excess, which was formed by the United States Department of Agriculture for Soil Conservation Service in 1972.

This model is related to input parameters including cumulative precipitation, soil cover, land use, and antecedent moisture. The SCS-CN is described from the equation as follows [25].

$$P_e = \frac{(P - I_a)^2}{P - I_a + S}$$

Equation 2

where: P_e accumulated precipitation excess at time t (runoff); *P* accumulated rainfall depth at time *t* (precipitation); *Ia* is the initial abstraction or initial loss; and *S* is potential maximum retention (mm). Through many experimental consequents of the SCS, a relationship of I_a and *S* had determined as:

$$I_a = 0.2S$$

Equation 3

Therefore, Equation 2 will be rewritten as:

$$P_e = \frac{(P - 0.2)^2}{P + 0.8S}$$

Equation 4

Besides, the S can't be calculated directly but the *S* is related to the *CN*:

$$S = \frac{25400}{CN} - 254$$

Equation 5

In which the *CN* for a watershed can be estimated as a function of LULC, soil type, and moisture. The *CN* values vary from 0 to 100, *CN*=100 for waterproof surfaces or water bodies, and *CN* <100 for natural surfaces [31]. Equation 6 represents calculating the composite *CN* value according to a watershed:

$$CN_{(cp)} = \frac{\sum_{i=1}^{n} A_i CN_i}{\sum_{i=1}^{n} A_i}$$

Equation 6

where: $CN_{(cp)}$ is the composite *CN*; *i* is an index of watersheds subdivisions of uniform LULC and soil type; A_i is the drainage area of subdivision *i*; CN_i is equivalent to each subdivided of the *CN*; *n* is the number of watersheds subdivisions. The *CN* has been tabulated by the SCS which is based on soil and LULC situation [25].

Direct-runoff model: In order to the basin lag, the research has applied the Snyder Unit hydrograph model [25], Synder proposed:

$$t_p = CC_t (LL_c)^{0.3}$$

Equation 7

In which t_p: the basin lag time (defined as the time difference between the centroid of the excess rainfall time and the flood peak time); C_t: basin coefficient (usually ranging from 1.8 ÷ 2.2 [32]); *L*: length of the mainstream from the outlet to the divide; L_c: length along the mainstream from the outlet to a point nearest the watershed centroid; *C*: a conversion constant of 0.75 for SI and 1.00 for foot-pound system [25].

Baseflow models (q_b): The study area has had a scarcity of information or data, therefore to calculate groundwater flow, the constant monthly baseflow method being for each time step of the modeling has been applied.

Routing model (Q_p-m^3/s): The Muskingum-Cunge method has been used to account for the flood wave movements across the river or reservoir sections, basing on the continuity equation and correlation between discharge and volume [25].

2.3.3 Model calibration and validation

Several statistical indices have been presented in the research for the performance assessment by determining the quality and reliability of simulation results, such as the Correlation coefficient-R, Nash-Sutcliffe simulation efficiency-NSE, Percentage bias-PBIAS, and Peak flow criterion-PFC [9] and [33].

3. Results and Discussion

3.1 LULC Change

Landsat satellite images of 2010, 2016, and 2020 are classified [1]. The LULC map containing the following six land-cover classes are made: agriculture, bare land, dense forest, open forest, urban/built-up, and water (Figure 2). The Kappa coefficient for the 2010 image is calculated as 0.75 [29] with 251 points which were used for images classification (dense forest - 46 points, open forest – 43 points, water – 33 points, urban/built-up – 52 points, bare land – 38 points, and agriculture – 39 points). Change analysis was done by calculating the areas of LULC in 2010 and then relating to the areas of LULC in 2020 as shown in Figure 2(d). The final LULC change for the years 2010 and 2020 along with the graphs of change analysis. In the period 2010 - 2016, the area of agricultural land and open forest land increased by 110.99 km^2 (40.1%) and 78.63 km^2 (6.2% per year), respectively.

Meanwhile, water decreased 41.1% per year, and dense forest decreased sharply by 211.88 km^2, equivalent to 27.3% per year. In the period 2016 - 2020, LULC has the strongest change in dense forest, continuing to decrease by 236.05 km^2, equivalent to 72.2% per year, bare land by 39.23 km^2 (19.7% per year), and agriculture by about 21.17 km^2 (5.8 % per year).

In the opposite direction, open forest increased in area by 261.67 km^2, equivalent to 16.2% per year, urban/built-up increased by 24.98 km^2 (9% per year). In the period 2010 – 2020, we can see that the dense forest, bare land, and water show a prominent decreased in 471.62 km^2, 60.31 km^2 and 15.33 km^2, respectively. Whereas the urban/built-up, agriculture, and open forest (mainly planted forests such as acacia species and eucalyptus) are likely to increase by 93.37 km^2, 152.01 km^2, and 400.61 km^2. These are influenced by urbanization [34], and Resolution on agricultural-rural development for the period 2016-2020 of Binhdinh province [35]. Furthermore, these dynamics are associated with government policy in 2016, "Protection and Development of production forest" is initiated by the central government, and most areas of Vietnam entered into the period of production forest to serve the economic development of ethnic minorities and farmers [36].

3.2 Generation of CN

The CN values of Laigiang river basin are obtained from LULC map and soil map. A soil map is processed to extract on the geological map to getting that the study area consists of seventeen types of land (Figure 3).

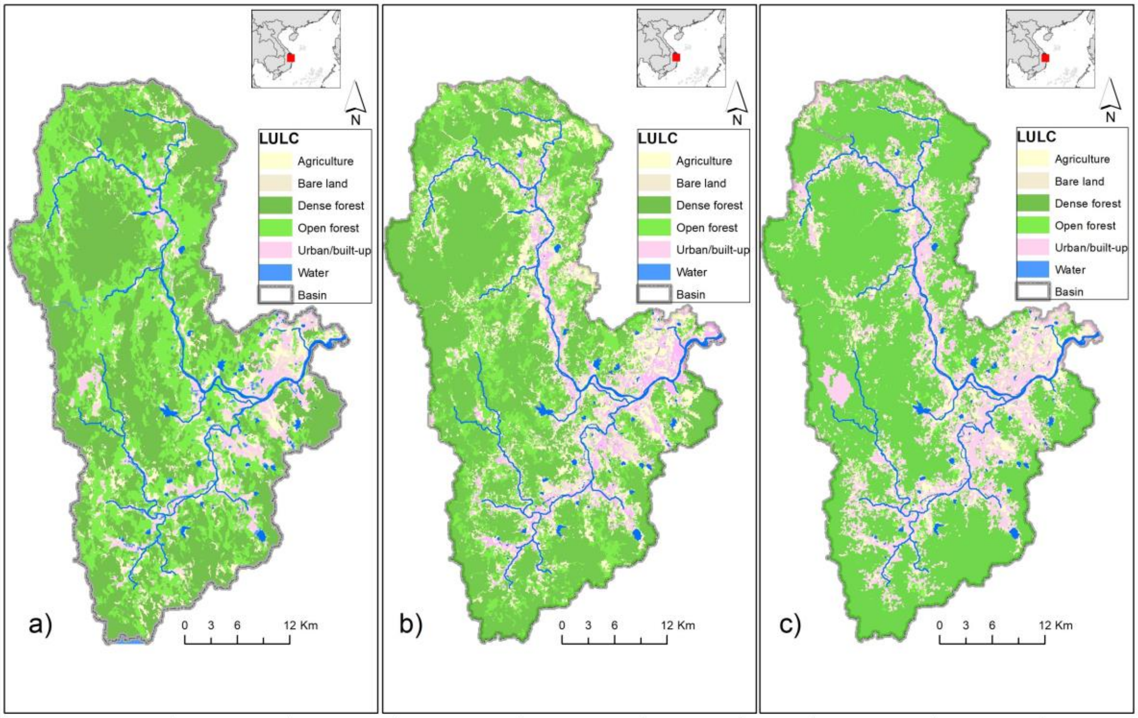

Land cover (km^2)	Agriculture	Bare land	Open forest	Dense forest	Urban/ built-up	Water	Total 2010	Decrease	Changes
Agriculture	20.82	7.57	42.84	4.08	7.18	0.52	**83.01**	62.19	89.82
Bare land	27.39	12.26	25.83	3.55	25.09	3.28	**97.40**	85.15	-17.33
Open forest	23.22	17.41	538.59	12.01	7.37	0.30	**598.90**	60.31	342.39
Dense forest	67.34	33.29	322.65	21.86	46.15	2.29	**493.48**	471.62	-447.93
Urban/built-up	29.87	6.99	8.69	3.74	51.61	2.85	**103.75**	52.14	41.23
Water	4.19	2.56	0.70	0.30	7.58	11.93	**27.26**	15.33	-6.09
Total 2020	**172.83**	**80.07**	**939.20**	**45.55**	**144.98**	**21.17**	**1403.80**		
Increase	152.01	67.82	400.61	23.69	93.37	9.24			

d)

Figure 2: LULC for the study area with (a) 2010, (b) 2016, (c) 2020 and (d) increase/decrease of the area in the period 2010-2020

ISSN: 1686-6576 (Printed) | ISSN 2673-0014 (Online) | © Geoinformatics International

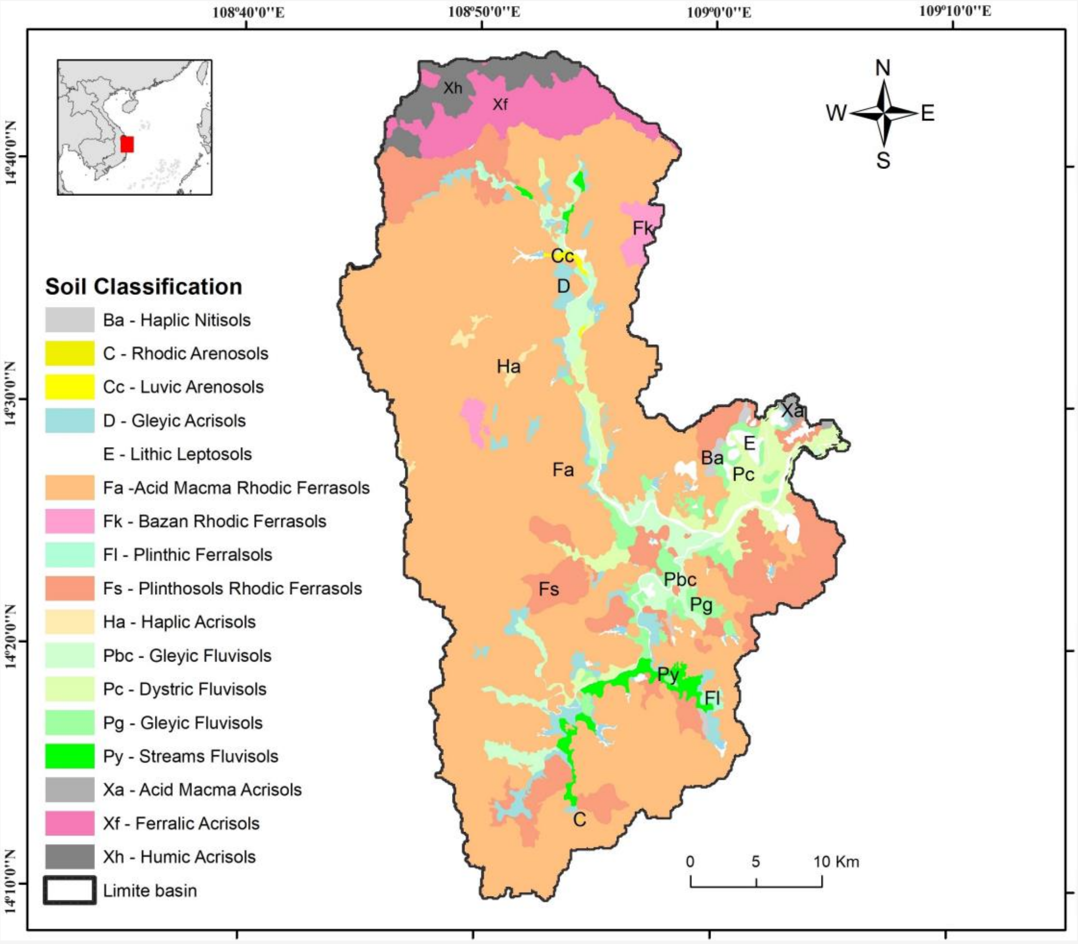

Figure 3: Soil classification of Laigiang river basin

Based on Equation 6, the average CN values are obtained for 2010, 2016, and 2020 in Laigiang river basin (Figure 4(a), 4(b), 4(c)). Figure 4(d) shows the average CN values change of each sub-basin. The average CN values tend to increase in the period 2010-2020. Typically, in the sub-basin, namely: L02 in the upstream of Laigiang river, the average CN values increase the most by 20.0% per year. In contrast, in the sub-basin, namely: LG05 increase by 7.6% per year. Raster maps of CN are generated as shown in Figure 4, which can give an explanation for the dark shades of black represent a higher value of average CN and therefore the higher runoff potential areas while the brighter colors (tsavorite green) represent lower runoff potential areas.

3.3 HEC-HMS Model Results

The HEC-HMS is used to simulate the hydrological processes in the catchment. The basin schematic, the flow direction data, location of hydrometric stations, and outlet in the Laigiang basin are built. The represent schematic of the basin consists of 09 sub-basins, junctions, reaches, and one outlet (Figure 5(a)). The mean area precipitation of Laigiang river basin: This study uses rainfall data of six observation stations (Anhoa, Bongson, Hoaian, Phumy, Hoainhon, and Vinhson) from the Binh Dinh Meteorological Department using two days of hourly rain-fall events from 15th to 16th of December 2016 at the study area. Equation 1, the Thiessen polygon networks and these six stations are used to obtain the mean area precipitation (Figure 5(b)). Figure 5(b) shows the mean area precipitation is about 218,8 mm on 15th December 2016 in the Laigiang river basin.

Losses by SCN CN: Based on Equation 4 and Equation 6 for flow loss estimated of Laigiang river basin in 2010, 2016, and 2020 have been shown in Table 1. In the sub-basins of L01, L02, L03, and L04 in the upstream where the forest area is predominant, the I_a index is always higher than the sub-basins of L09 and L06 in the downstream and estuary (Table 1).

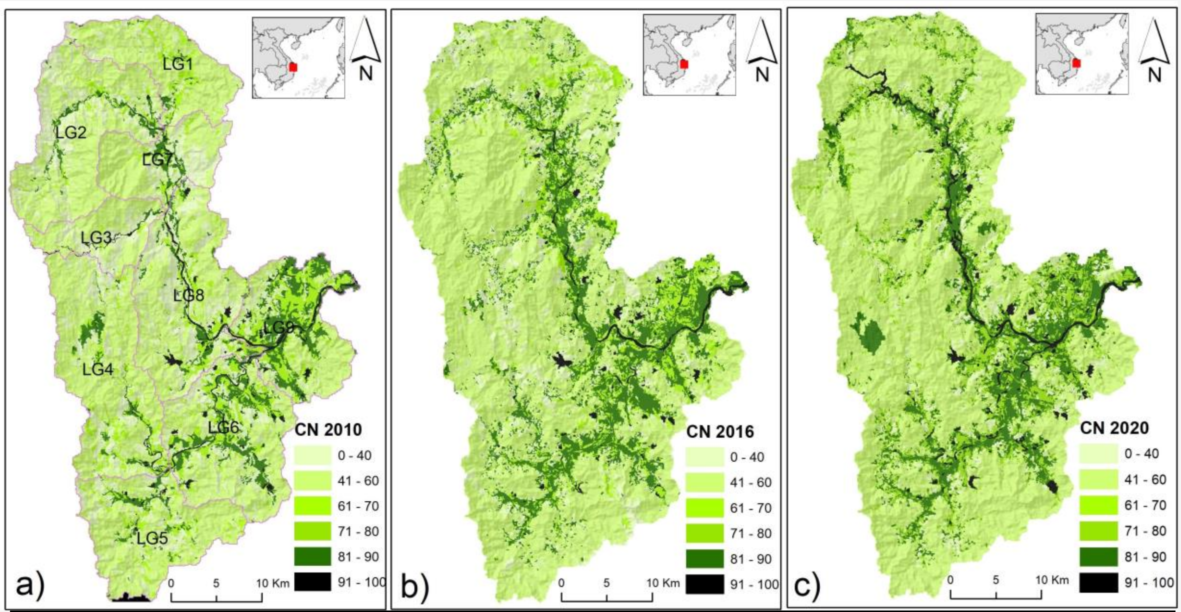

d)

Sub-basin	A_i (km^2)	CN_{cp}			Increasing Rate (%)
		2010	2016	2020	
L01	114.4	55.1	57.3	60.3	8.6
L02	197.1	51.5	56.7	61.8	20.0
L03	71.7	51.3	56.6	60.0	17.0
L04	217.8	55.5	56.6	61.7	11.2
L05	161.5	60.9	61.7	65.5	7.6
L06	192.2	74.9	79.4	83.4	11.3
L07	96.2	58.7	65.7	68.5	16.7
L08	204.7	70.8	77.6	81.0	14.4
L09	148.2	82.9	85.8	90.1	8.7

Figure 4: Average CN value in 2010 (a) 2016 (b) 2020 (c) and (d) Percentage increase in Laigiang river basin

Table 1: Estimating initial loss and runoff transform of the Laigiang river

Subbasin	A_i (km^2)	Parameters				Potential maximum retention-S			Initial loss-I_a		
		L_{ci} (km)	L_i (km)	C_t	Y_p (h)	2010	2016	2020	2010	2016	2020
L01	114.4	7.60	10.08	0.70	1.93	203.7	189.3	167.2	40.7	37.9	33.4
L02	197.1	10.00	20.27	0.60	2.21	239.2	194.0	157,0	47.8	38.8	31.4
L03	71.7	5.00	1.84	0.60	0.88	241.1	194.8	169.3	48.2	39.0	33.9
L04	217.8	12.40	18.60	0.70	2.69	203.7	194.8	157.7	40.7	39.0	31.5
L05	161.5	7.60	5.89	0.60	1.41	163.1	157.7	133.8	32.6	31.5	26.8
L06	192.2	10.40	25.76	0.40	1.61	85.1	65.9	50.6	17.0	13.2	10.1
L07	96.2	5.70	11.73	0.50	1.32	178.7	132.6	116.8	35.7	26.5	23.4
L08	204.7	10.10	25.18	0.40	1.58	104.8	73.3	59.6	21.0	14.7	11.9
L09	148.2	8.00	15.89	0.40	1.28	52.4	42.0	27.9	10.5	8.4	5.6

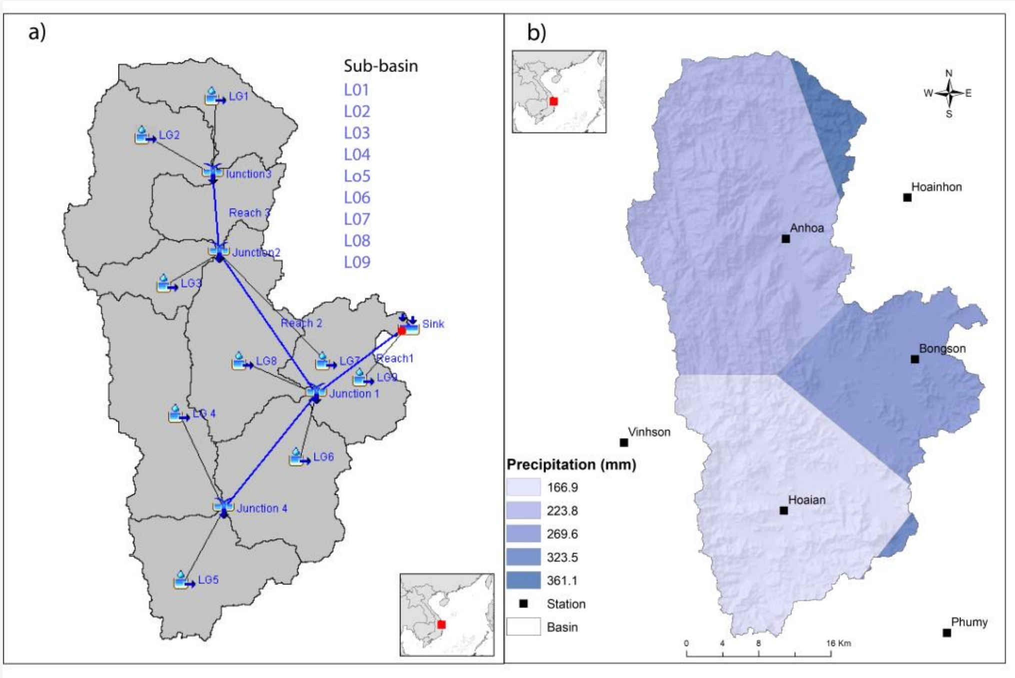

Figure 5: (a) Schematic model of the HEC-HMS and (b) Precipitation on 15th December 2016

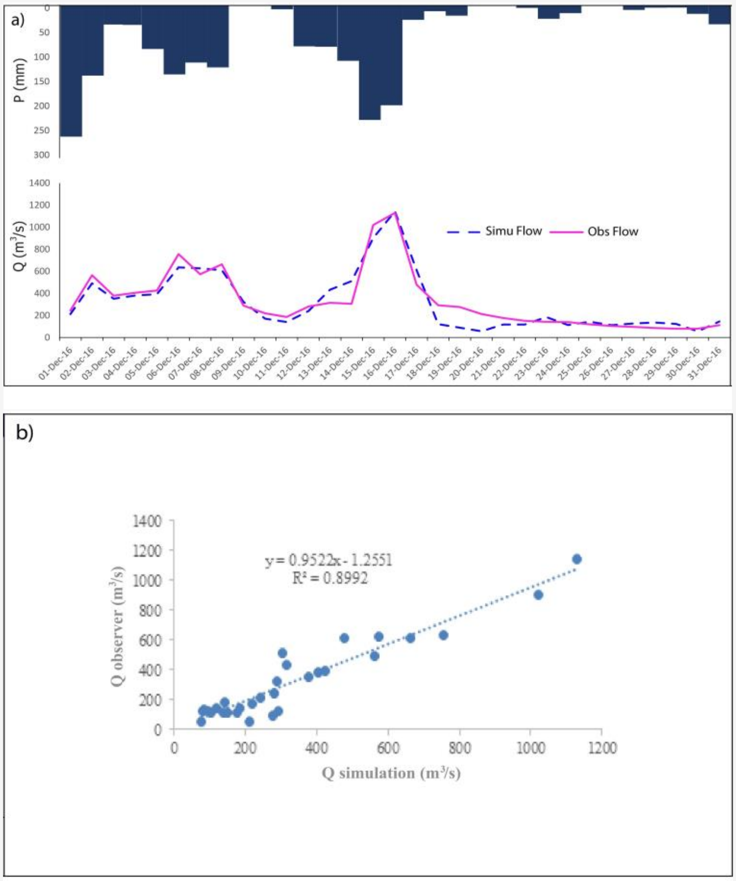

Figure 6: Observed and simulation for flood event in the 16th December 2016 in Anhoa station

However, I_a tends to decrease gradually in the period 2010-2020, typically sub-basin of L02 has the largest decrease from 47.8 to 31.4 (52% per year). This reflects the decreasing capacity of water in the rainy season in upstream of the Laigiang river basin. Estimation of the model parameters: This study uses Equation 7 and GIS to determine distances that have been the input parameters for estimating runoff transformation (Table 1).

Coefficient of Manning: Beds of Natural runoffs comprise unclassified sand, gravels, and rocks, so the bottom roughness of rivers is not uniform, resulting into effect on the water flow [37]. The roughness coefficient of the bed makes it possible to have a model that is closest to reality by taking into account the speed of the water on the bottom and on the banks [38]. Hence, the Manning roughness coefficient-n has been determined for the research area by using Strickler's formula (K = 1/n). This is an empirical coefficient that depends on many factors, including the surface roughness (nature of the vegetation cover and bare surfaces) and sinuosity [37] and [39].

3.4 Simulation of the Runoff on the Historical Flood Event

Figure 6 shows the daily observed and computed outflow in December 2016 of Laigiang river basin. The flood peak appeared on the 16th of December 2016 during calibration and validation (Figure 6 (a)). The statistical performance was satisfactory according to the daily R^2 = 0.89, NSE= 0.99, PBIAS = 0.05 and PFC = 3.73 (Figure 6 (b)). The statistical results showed good agreement by comparing the computed outflow with the simulation, and the parameters calibrated for outflow of the model could be used to simulate every sub-watershed as well as different LULCs scenarios in the study area.

3.5 Impact of Land Cover Changes on the Flood Volume

The LULC of 2016 gathered from the Laigiang river basin is used in the initial run of the HEC-HMS models, which are created in December 2016. In order to assess the influence of LULC change on the flow, we use hydrometeorological data measured at Anhoa station in December 2016 for two scenarios LULCs 2010 and 2020, respectively in terms of topography, rainfall, and soil types unchanged. Figure 7 display the hydrographs and peak discharge in scenarios LULCs 2010 and 2020 of Laigiang river basin using the HEC-HMS model showing the outflows of rainfall events in December 2016. We can confirm that when LULC change in Laigiang river basin according to the trend of forest conversion to the low-density vegetation, i.e. development areas, agricultural regions, and urbanization, which has influenced the increased peak discharge of 1149 m^3/s under the LULC 2020 scenario compared to the LULC in 2016 is 1130 m^3/s. This study is based on the HEC-HMS model to determine the peak discharge changes of sub-basin. Figure 8(a) shows that the peak discharge value of sub-basin of LG4 upstream of the Laigiang river basin (a tributary of Kim Son) under the LULC 2010 scenario is 327 m^3/s and the LULC 2020 scenario is 334 m^3/s, an increase of 2.1 % per year.

Meanwhile, the peak discharge value of sub-basin number LG9 in the estuary area, which is adjacent to the East Sea, did not change much between the LULC 2010 scenario (221 m^3/s) and the LULC 2020 scenario (222 m^3/s), an increase of 0.3% per year.

Figure 8(b) shows that the outcome of land cover changes on the rate of flood volume corresponds to the LULCs scenarios of 2010 and 2020 led to the enhancement of flood volume. This increase in flood volume is possibly owing to the alteration to urbanization with the new establishment of Hoainhon town (2020) in the downstream area; agricultural area (i.e. corn, cassava, mango, and mixed agriculture) to serve the policy of agricultural restructuring forest quality declines due to the development of industrial plantations (i.e. acacia and eucalyptus) [40]; and especially deforestation of 43.7 ha in 2017 as well as building an 89.8 million m^3 Dongmit dam for irrigation reservoir built-in 2020 in An Lao district is located upstream in the Laigiang river basin. Through the analysis results, there are many causes of flooding at the study area, which the cause is the influence of climate change caused unusually heavy rain over in this river basin. In addition, under the influence of activities in the process of socio-economic development such as riverside infrastructure development has narrowed the river bed, the destruction of the primary forest upstream, conversion of forest purpose from special-use to production forest, urbanization of the Laigiang estuary, these will make the more historical floods in future. On the basis of LULC scenarios in 2010 and 2020 compared with the flood event in December 2016, there are differences in flood discharge between sub-basins. Sub-basins with large vegetation cover play a great role in regulating flood flows and conversely, sub-basins mainly in urban areas have very poor surface water storage capacity.

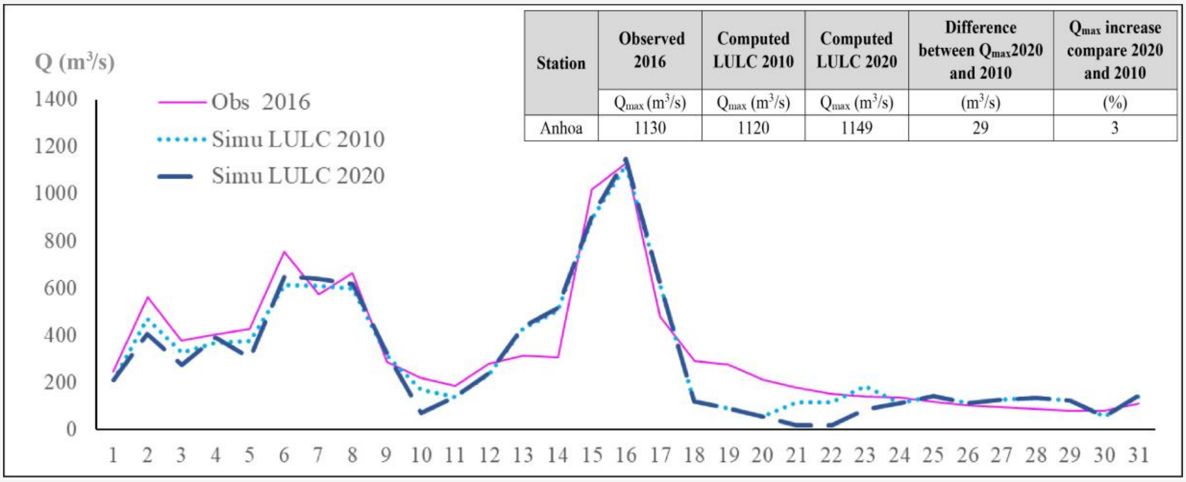

Station	Observed 2016	Computed LULC 2010	Computed LULC 2020	Difference between Q_{max}2020 and 2010	Q_{max} increase compare 2020 and 2010
	Q_{max} (m^3/s)	Q_{max} (m^3/s)	Q_{max} (m^3/s)	(m^3/s)	(%)
Anhoa	1130	1120	1149	29	3

Figure 7: The scenario of peak discharge at Anhoa hydrological station corresponding to LULCs 2010 and 2020 for flood event

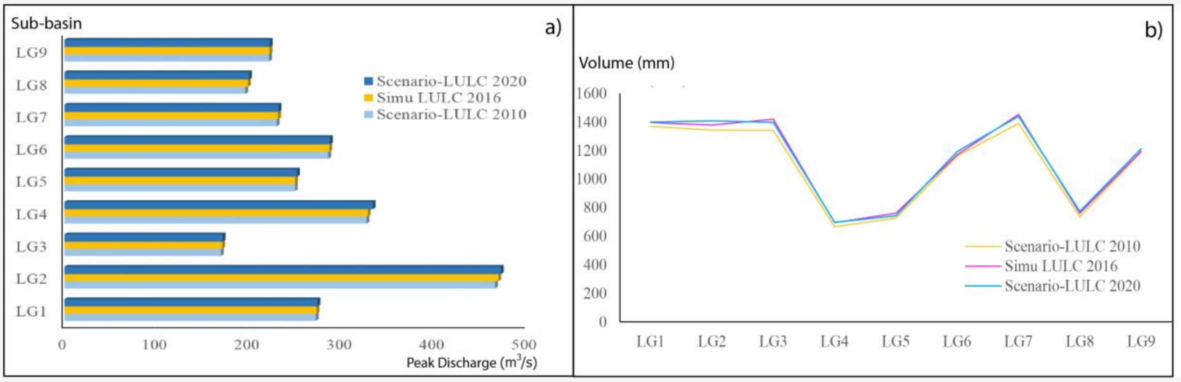

Figure 8: (a) Peak discharge changes of sub-basins and (b) - Comparison of the total volume change under land cover/land-use scenarios of LULCs 2010 and 2020

It can be affirmed that frequent flooding in this basin is a big problem in the coming time, so a new approach is needed to reduce the risk of flooding by continuing to improve the quality of natural forest cover in the upstream sub-basins, the conversion of forests to production forests should be limited in the middle sub-basins, and the use of agricultural land for urban use should be minimized the industrialization and development of industrial zones in downstream of the river basin.

4. Conclusion

This study provides the assessment of the influence of LULC change on the runoff changes using the spatial temporal regional remote sensing, GIS and HEC-HMS under the rainfall events in December 2016 at the Laigiang river basin. The following conclusions and key findings can be summarised:

- The area of dense forest in the upper reaches of the river basin tends to decrease gradually and in contrast, the open forest with mainly acacia and eucalyptus trees tends to increase in the period 2010-2020. This has affected the quality of forests, reduced water retention, increased the risk of flooding, affected groundwater shortages, and risked drought in the dry season.

- CN value has a close relationship with the surface flow of the river basin. The sub-basins with low vegetation cover, high concretization (typically sub-basins of 06, 08 and 09) corresponds to CN reaching values close to 100, which is proportional to the increased surface runoff. In contrast, high-coverage sub-basins where there is a lot of forest (specifically as sub-basins of 01, 02, 03 and 04) correspond to CN values approaching 40 and surface runoff decreases.

This helps local authorities to realize clearly the role of forest cover in reducing the risk of drought and regulating flood flows in the river basin. The local authorities' decisions on land use planning should limit the leveling of agricultural land in the lower river basin to convert the purpose to urban land.

- The use of HEC-HMS showed that changes in LULC led to fundamental changes in the infiltration/water loss response to precipitation events, particularly during the rainy season, where runoff flows tend to higher trend under the cover scenarios in 2010 and 2020 compared to 2016.

- The accuracy of HEC-HMS depends greatly on LULC and riverbed topography. Therefore, in the future, it is necessary to use higher resolution satellite images to determine LULC and use multi-beam echoes to determine riverbed topography, using more typical radar satellite images such as Sentinel-1 to build a DEM model of the river basin. In addition, rainfall monitoring systems from the ground as well as from satellite images need to be combined to increase the accuracy of the HEC-HMS model.

Acknowledgements
The authors would like to thank Quynhon University, Vietnam, with code being B2020-DQN-03 provided financial support and data for this study.

References

[1] Sanchayita, R. and Jyotirmoy, S., (2021). Climate Change and Flood Risk, Global Climate Change. *Global Climate Change*, 321-339. https://doi.org/10.1016/B978-0-12-8229286.0 0012-5.

[2] Bruijnzeel, L. A., 2004, Hydrological Functions of Tropical Forests: Not Seeing the Soil for the Trees?. *Agriculture, Ecosystems and Environment*, Vol. 104, 185–228. https://doi.org/10.1016/j.agee.2004.01.015.

[3] Edivaldo Afonso de Oliveira, S., Madson Tavares, S., Thomás Rocha, F., Lorena Conceição, P. de A., Cleber, A. dos S., Aline Maria, M. de L., Vicente, de P. R. da S., Francisco, de A. S. de S. and Dênis Jose, C. G., (2021). Impacts of land Use and Land Cover Changes on Hydrological Processes and Sediment Yield Determined Using the SWAT Model. *International Journal of Sediment Research*, Vol. 37(1), 54-69. https://doi.org/10.1016/j.ijsrc.2021.04.002.

[4] Lajoie, F., Assani, A. A., Roy, A. G. and Mesfioui, M., (2007). Impacts of Dams on Monthly Flow Characteristics. The Influence of Watershed Size and Seasons. *Journal of Hydrology*, Vol. 334, 423–439. https://doi.org/10.1016/j.jhydrol.2006.10.019.

[5] Tran, B. and Doan, N., (2017). Relationship between Watershed Characteristics and Flow Rate of Typical Watersheds in Vietnam. *Forest Science Journal Vietnam*, Vol. 2, 1-10.

[6] Mingteh, C., (2012). *Forest Hydrology: An Introduction to Water and Forests, in: Forest Hydrology: An Introduction to Water and Forests*. 3rd Edition. CRC Press, Boca Raton, 1-598.

[7] Sun, G., Zhou, G., Zhang, Z., Wei, X., McNulty, S. G. and Vose, J., (2005). *Forest and Water Relationships: Hydrologic Implications of Forestation Campaigns in China*. Nanchang, Jiangxi Province, China. *Scientific Journal (JRNL)*, 1-32.

[8] Hu, Y., Nacun, B., Zhen, L. and Zhuang, D., (2019). Assessment of Land-Use and Land-Cover Change in Guangxi, China. *Scientific Reports*, Vol. 9(1), 1-13. https://doi.org/10.1038/s41598-019-38487-w.

[9] Huang, X. D., Shi, Z. H., Fang, N. F. and Li, X., (2016). Influences of Land Use Change on Baseflow in Mountainous Watersheds. *Forests*, Vol. 7, 1-16. https://doi.org/10.3390/f7010016.

[10] Owuor, S. O., Butterbach-Bahl, K., Guzha, A. C., Jacobs, S., Merbold, L., Rufino, M. C., Pelster, D. E., Díaz-Pinés, E. and Breuer, L., (2018). Conversion of Natural Forest Results in a Significant Degradation of Soil Hydraulic Properties in the Highlands of Kenya. *Soil and Tillage Research*, Vol. 176, 36–44. https://doi.org/10.1016/j.still.2017.10.003.

[11] Mihnea Cristian, P. and Diaconu, D., (2019). *Effects of Deforestation on Flooding in the Moldova River Basin. 2019 "Air and Water – Components of the Environment" Conference Proceedings, Cluj-Napoca, Romania*, 129-136.

[12] Younis, S. M. Z. and Ammar, A., (2018). Quantification of Impact of Changes in Land Use-Land Cover on Hydrology in the Upper Indus Basin, Pakistan. *The Egyptian Journal of Remote Sensing and Space Science*, Vol. 21, 255–263. https://doi.org/10.1016/j.ejrs.2017.11.001.

[13] Meyfroidt, P., Vu, T. P. and Hoang, V. A., (2013). Trajectories of Deforestation, Coffee Expansion and Displacement of Shifting Cultivation in the Central Highlands of Vietnam. *Global Environmental Change*, Vol. 23, 1187–1198. https://doi.org/10.1016/j.gloenvcha.2013.04.005.

[14] Ali, J., Benjaminsen, T. A., Hammad, A. A. and Dick, Ø. B., (2005). The Road to Deforestation: An Assessment of Forest Loss and its Causes in Basho Valley, Northern Pakistan. *Global Environmental Change*, Vol. 15, 370–380. https://doi.org/10.1016/j.gloenvcha.2005.06.004.

[15] Yang, S., Büttner, O., Jawitz, J. W., Kumar, R., Rao, P. S. C. and Borchardt, D., (2019). Spatial Organization of Human Population and Wastewater Treatment Plants in Urbanized River Basins. *Water Resources Research*, Vol. 55, 6138–6152. https://doi.org/10.1029/2018WR024614.

[16] Nguyen, M. T., Sebesvari, Z., Souvignet, M., Bachofer, F., Braun, A., Garschagen, M., Schinkel, U., Yang, L. E., Nguyen, L. H. K., Hochschild, V., Assmann, A. and Hagenlocher, M., (2021). Understanding and Assessing Flood Risk in Vietnam: Current Status, Persisting Gaps, and Future Directions. *Journal of Flood Risk Management*, Vol. 14(2). https://doi.org/ 10.1111-/jfr3.12689.

[17] Laux, P., Nguyen, P. N. B., Cullmann, J. and Kunstmann, H., (2017). Impacts of Land-Use/Land-Cover Change and Climate Change on the Regional Climate in the Central Vietnam. Nauditt, A., Ribbe, L. (Eds.), Land Use and Climate Change Interactions in Central Vietnam: LUCCi. *Water Resources Development and Management*. Springer, Singapore, 143–151. https://doi.org/10.1007/978-981-10-2624-9_9.

[18] Usman, M., Liedl, R., Shahid, M. A. and Abbas, A., (2015). Land Use/Land Cover Classification and Its Change Detection Using Multi-Temporal MODIS NDVI Data. *J. Geogr. Sci.*, Vol. 25, 1479–1506. https://doi.org/10.1007/ s11442-015-1247-y.

[19] Hong, N., Bich, N., Le, T., Nguyen, H., Nguyen, L. and Địa, K., (2015). Effect of Land Use Change on Water Discharge in Vu Gia – Thu Bồn Watershed. *Journal of Vietnam Geology* A, Vol. 351, 49–59.

[20] Latchininsky, A., Piou, C., Franc, A. and Soti, V., (2016). Applications of Remote Sensing to Locust Management, in: Baghdadi, N., Zribi, M. (Eds.). *Land Surface Remote Sensing*, 263–293. https://doi.org/10.1016/B978-1-78548105-5.50008-6.

[21] [29] Saadatkhah, N., Haddad Tehrani, M. R., Mansor, S., Khuzaimah, Z., Kassim, A. and Saadatkhah, R., (2016). Impact Assessment of Land Cover Changes on the Runoff Changes on the Extreme Flood Events in the Kelantan River Basin. Arabian *Journal of Geosciences,* Vol. 9, 1-17. https://doi.org/10.1007/s12517-016-271 6-z.

[22] Thakur, J. K., Singh, S. K. and Ekanthalu, V. S., (2017). Integrating Remote Sensing, Geographic Information Systems and Global Positioning System Techniques with Hydrological Modeling. *Appl. Water* Sci., Vol. 7, 1595–1608. https://doi.org/10.1007/s13201-016-0384-5.

[23] Huong, D. T., Tan, T. Q., Dung, T. S., Don, T. V., Dung, L. V., Quynh, N. N. and Thiep, N. T., (2005). *Hydrometeorological Characteristics of Binhdinh Province*. The Science and Technology Project of Binhdinh Province, Vietnam.

[24] Sumarauw, J. S. F. and Ohgushi, K., (2012). Analysis on Curve Number, Land Use and Land Cover Changes and the Impact to the Peak Flow in the Jobaru River Basin, Japan, *International Journal of Civil & Environmental Engineering*, Vol. 12, 1-7.

[25] USACE, (2000). *HEC-HMS Technical Reference Manual*. Arlen D. Feldman. ed. US Army Corps of Engineers, Institute for Water Resources, Hydrologic Engineering Center.

[26] Mahendra, H. N., Shivakumar, B. R. and Praveen, J., (2015). Pixel-based Classification of Multispectral Remotely Sensed Data Using Support Vector Machine Classifier. *IJIREEICE*, Vol. 3, 94–98.

[27] Adewuyi, K., Page, Babatunde, A. and Aderinkomi, S., (2017). Remote Sensing and GIS Application in Image Classification and Identification Analysis. *Journal of Research in Environmental and Earth Science,* Vol. 3, 55–66.

[28] Jensen, J. R., (1995). *Introductory Digital Image Processing: A Remote Sensing Perspective*. Prentice Hall, Upper Saddle River, NJ. https://www.gbv.de/dms/goettingen/186021380.pdf.

[29] Giraldo, M. A., Chaudhari, L. S. and Schulz, L. O., (2012). Land-Use and Land-Cover Assessment for the Study of Lifestyle Change in a Rural Mexican Community: The Maycoba Project. *International Journal of Health Geographics*, Vol. 11, https://doi.org/10.1186/1476-072X-11-27.

[30] Schumann, A. H., (1998). *Thiessen PolygonThiessen Polygon*. Encyclopedia of Hydrology and Lakes, Encyclopedia of Earth Science. Springer Netherlands, Dordrecht, 648–649.

[31] Coulson, M., van Deursen, W. P. A., Danson, F. M., Plummer, S. E., Williams, J. and Mather, P. M., (1996). Geographical Information Systems and Dynamic Models. *The Geographical Journal*, Vol. 162(2), 219-220.

[32] Philip, B, B., Wayne, C, H. and Baxter E, V., (2019). *Hydrology and Floodplain Analysis*, 6th Edition, Published by Pearson.

[33] Gupta, H., Sorooshian, S. and Yapo, P., (1999). Status of Automatic Calibration for Hydrologic Models: Comparison with Multilevel Expert Calibration. *Journal of Hydrologic Engineering*, Vol. 4, 135-143. https://doi.org/10.1061-/(ASCE)1084-0699(1999)4:2(135).

[34] Ha, N. M., Le, N. D. and Trung-Kien, P., (2019). The Impact of Urbanization on Income Inequality: A Study in Vietnam. *Journal of Risk and Financial Management*, Vol. 12(3), https://doi.org/10.33-90/jrfm12030146.

[35] Decision No 699, N. 699, (2017). *Implementation plan of the Action Plan of Provincial Party Committee Implements the Resolution of the 12th Party Congress and Resolution the 19th Congress of the Provincial Party Committee on Agriculture and Rural Development in Binhdinh province in the Period 2016-2020*. People’s Committee of Binhdinh Province, Vietnam.

[36] Decision No 38, (2016). *Issuing Some Policies on Forest Protection, Development and Investments in Infrastructure Support, Against Public Utilities to Agriculture and Forestry Companies (No. 38/2016/QD-TTg)*. Prime Minister, Vietnam.

[37] Chanson, H., (2004). *The Hydraulics of Open Channel Flow: An Introduction Basic Principles, Sediment Motion, Hydraulic Modelling, Design of Hydraulic Structures*. Hydraulics of Open Channel Flow (Second Edition). Elsevier Butterworth-Heinemann, Oxford, 1-634.

[38] Lahsaini, M. and Tabyaoui, H., 2018, Modelisation Hydraulique Mono Dimen-sionnel Par HEC RAS, Application Sur L’oued Aggay (Ville De Sefrou). *European Scientific Journal, ESJ*, Vol. 14(18). https://doi.org/10.19044/esj.2018.v14n18p110.

[39] Tinkler, K. J., (1997). Critical Flow in Rockbed Streams with Estimated Values for Manning’s n. *Geomorphology*, Vol. 20, 147–164.

[40] Kartodihardjo, H. and Supriono, A., (2000). The Impact of Sectoral Development on Natural Forest Conversion and Degradation: The Case of Timber and Tree Crop Plantations in Indonesia. *Occasional Paper*, Vol. 26(E), 1–17. https://doi.org/10.17528/cifor/000628.